Bone Reports 20 (2024) 101725

Contents lists available at ScienceDirect

Bone Reports

journal homepage: www.elsevier.com/locate/bonr

Case Report

Burosumab for the treatment of cutaneous-skeletal hypophosphatemia syndrome

Lillian Abebe [a], Kim Phung [a,b], Marie-Eve Robinson [b,c], Richelle Waldner [d], Sasha Carsen [b,e], Kevin Smit [b,e], Andrew Tice [b,e], Joanna Lazier [f,g], Christine Armour [f,g], Marika Page [a], Saunya Dover [a], Frank Rauch [h,i], Khaldoun Koujok [a,j], Leanne M. Ward [a,b,c,*]

[a] The Ottawa Pediatric Bone Health Research Group, Children's Hospital of Eastern Ontario Research Institute, 401 Smyth Road, Ottawa, ON K1H 8L1, Canada
[b] Department of Pediatrics, Faculty of Medicine, University of Ottawa, 550 Cumberland St, Ottawa, ON K1N 6N5, Canada
[c] Division of Endocrinology and Metabolism, Department of Pediatrics, Children's Hospital of Eastern Ontario, 401 Smyth Road, Ottawa, ON K1H 8L1, Canada
[d] Department of Pediatrics, University of Alberta, 116 St & 85 Av, Edmonton, AB T6G 2R3, Canada
[e] Department of surgery, Children's Hospital of Eastern Ontario, 401 Smyth Road, Ottawa, ON K1H 8L1, Canada
[f] Department of Genetics, Children's Hospital of Eastern Ontario, 401 Smyth Road, Ottawa, ON K1H 8L1, Canada
[g] Department of Medical Genetics and Genomics, Faculty of Medicine, University of Ottawa, 550 Cumberland St, Ottawa, ON K1N 6N5, Canada
[h] Shriners Hospital for Children, 1003 Decarie Blvd, Montréal, QC H4A 0A9, Canada
[i] Department of Pediatrics, Faculty of Medicine and Health Sciences, McGill University, 805 rue Sherbrooke O, Montréal, Quebec H3A 0B9, Canada
[j] Department of Medical Imaging, Children's Hospital of Eastern Ontario, 401 Smyth Road, Ottawa, ON K1H 8L1, Canada

ARTICLE INFO

Keywords:
Cutaneous-skeletal hypophosphatemia syndrome
Fibroblast growth factor-23
Hypophosphatemic rickets
Burosumab
Conventional treatment
Child

ABSTRACT

Cutaneous-skeletal hypophosphatemia syndrome (CSHS) is a rare bone disorder featuring fibroblast growth factor-23 (FGF23)-mediated hypophosphatemic rickets. We report a 2-year, 10-month-old girl with CSHS treated with burosumab, a novel human monoclonal antibody targeting FGF23. This approach was associated with rickets healing, improvement in growth and lower limb deformity, and clinically significant benefit to her functional mobility and motor development. This case report provides evidence for the effective use of FGF23-neutralizing antibody therapy beyond the classic FGF23-mediated disorders of X-linked hypophosphatemia and tumor-induced osteomalacia.

1. Introduction

Cutaneous-skeletal hypophosphatemia syndrome (CSHS) is a rare bone disorder featuring skeletal and skin manifestations, caused by mosaic somatic activating *RAS* family pathogenic variants with mosaic effects (Lim et al., 2016). CSHS is characterized by the overproduction of fibroblast growth factor-23 (FGF23), which is secreted by osteocytes in affected dysplastic bones (Ovejero et al., 2023). FGF23 causes inhibition of renal absorption and gastrointestinal absorption of phosphate by lowering sodium phosphate cotransporter activity and limiting 1,25-dihydroxyvitamin D ($1,25(OH)_2D$) synthesis (Lim et al., 2016). Together, these biochemical aberrations result in hypophosphatemia, causing bone pain, rickets, long bone deformity, as well as impaired growth and mobility (Ovejero et al., 2016; Lim et al., 2016).

Conventional treatment of CSHS with phosphate supplementation and active vitamin D does not directly address the FGF23 over-expression (Lim et al., 2014). While phosphate supplementation brings about temporary increases in serum phosphorus levels, it also increases FGF23 production, which ultimately perpetuates the renal phosphate-wasting and fails to successfully treat rickets. Burosumab is a fully human monoclonal antibody, given subcutaneously every two weeks in children, that neutralizes FGF23. Burosumab was recently shown to be superior to conventional therapy in a phase 3 randomized controlled trial in children with X-linked hypophosphatemia (XLH), another childhood-onset condition linked to FGF23 overproduction (Imel et al., 2019).

Burosumab has been approved by numerous health authorities globally for the treatment of XLH and tumor-induced osteomalacia; however, there have been no pivotal trials and thereby a lack of formal approval for burosumab in other FGF23-mediated hypophosphatemic

* Corresponding author at: The Ottawa Pediatric Bone Health Research Group, Children's Hospital of Eastern Ontario Research Institute, 401 Smyth Road, Ottawa, ON K1H 8L1, Canada.
E-mail address: lward@cheo.on.ca (L.M. Ward).

https://doi.org/10.1016/j.bonr.2023.101725
Received 9 August 2023; Received in revised form 1 November 2023; Accepted 10 November 2023
Available online 11 November 2023

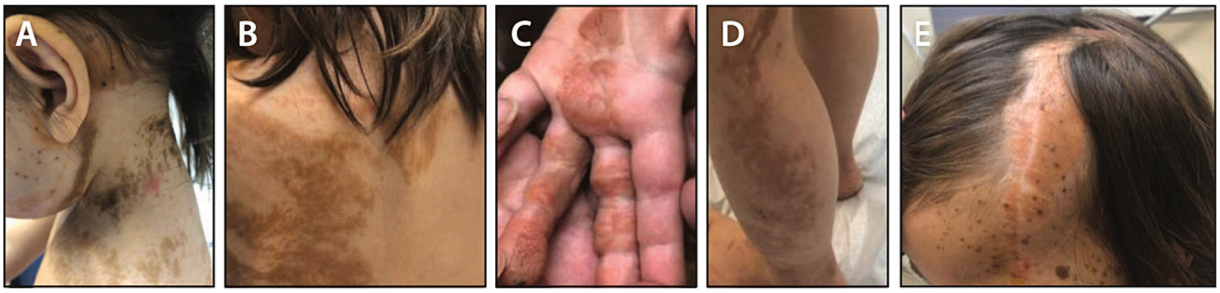

Fig. 1. Pictures of the patient's extensive left-sided nevi at diagnosis of cutaneous-skeletal hypophosphatemia syndrome on the neck (A), back (B), hand (C), leg (D), and head (E).

conditions. Here we describe the off-label use of burosumab in a young girl with CSHS, prescribed to optimize her management in the setting of an inadequate clinical response to conventional phosphate supplementation and active vitamin D therapy. The primary objective of this report was to discuss the dose and treatment response to anti-FGF23 antibody therapy in a child with moderate to severe CSHS.

2. Results

2.1. Case presentation

The patient was diagnosed at 4 months of age with linear sebaceous nevi characterized by extensive, strictly left-sided nevi on the neck, back, hand, leg, and head (Fig. 1). The nevi were partially surgically excised at 1 year and 4 months of age, with follow-up surgery a month later due to wound dehiscence. Genetic testing from excised tissue,

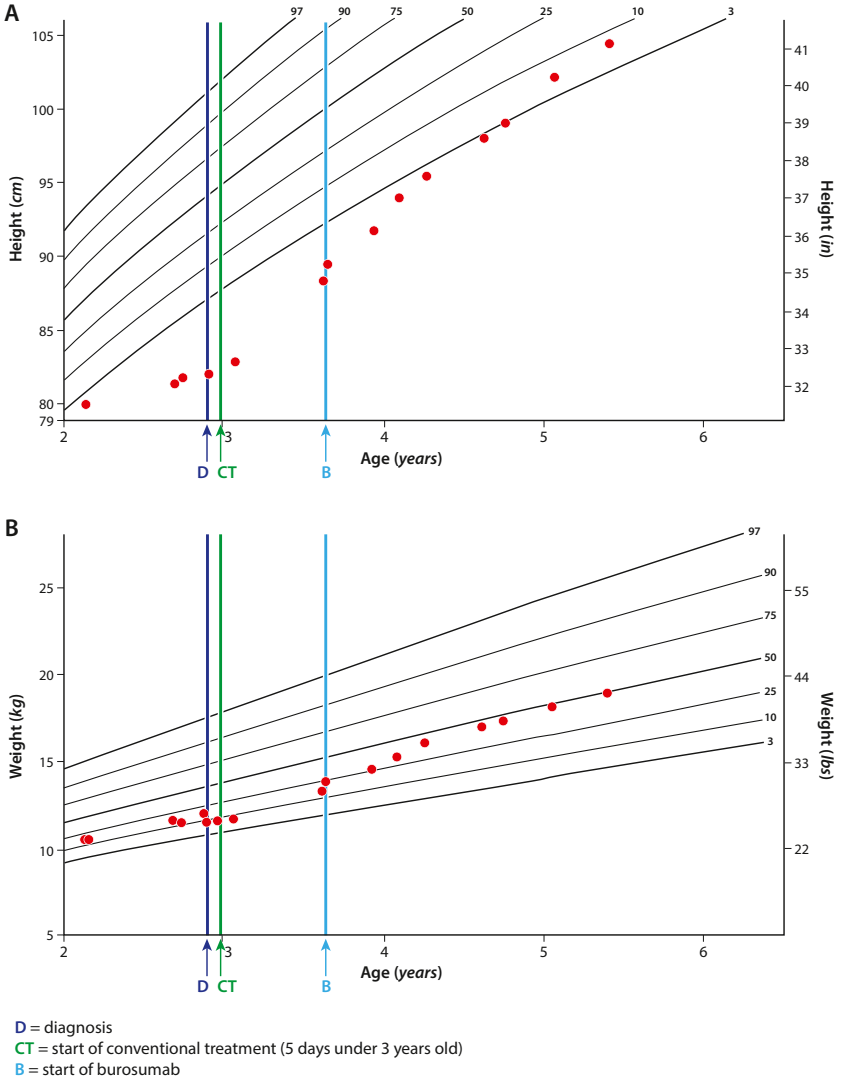

Fig. 2. Height (A) and weight (B) growth charts, with vertical lines indicating the time of diagnosis (purple), the start of conventional treatment (green), and the start of burosumab (light blue).

Table 1
Biochemical parameters at diagnosis in a child with cutaneous-skeletal hypophosphatemia syndrome.

Biochemical parameter	Result[a]	Normal range[b]
Serum phosphate (mmol/L) = low	**0.82**	**1.27–2.01**
Serum ionized calcium (mmol/L)	1.19	1.16–1.36
Serum PTH (pmol/L)	4.3	1.2–6.3
Serum 1,25(OH)$_2$D (pmol/L) = slightly high	**220**	**48–190**
Serum ALP (U/L)	295	145–324
Serum 25(OH)D (nmol/L)	91.1	50–250
Serum C-terminal FGF23 (RU/mL) = inappropriately normal	**63**	**19–114**
Urinary calcium/creatinine ratio (mmol/L/mmol/L)	0.10	0.08–0.60
Tubular reabsorption of phosphate (%) = inappropriately normal	**87.9**	**78–91**
Tubular maximum reabsorption of phosphate/glomerular filtration rate (mmol/L) = low	**0.72**	**1.15–2.44**

Abbreviations: 1,25(OH)$_2$D = 1,25-dihdroxyvitamin D; 25(OH)D = 25-hydroxyvitamin D; ALP = alkaline phosphatase; FGF23 = fibroblast growth factor-23; PTH = parathyroid hormone.

[a] Bolded results indicate values outside of the normative range or abnormal in the context of hypophosphatemia.

[b] Normative range for age and sex.

including a Noonan and RASopathy next-generation sequencing (NGS) custom panel of 31 genes, which included *AKT1*, *AKT2*, *AKT3*, *FGFR3*, *PIK3CA*, *PIK3R2*, and *PTEN* genes (performed by Fulgent Genetics, Temple City, California) and chromosomal microarray (SNP oligonucleotide array, human genome build 19), did not identify any pathogenic nor copy number variants.

At the age of 2 years and 10 months, the patient sought medical attention due to bone pain causing functional impairment that was associated with poor growth and limb deformity. Her anthropometric parameters were below average (weight 25th percentile, height below 3rd percentile) with poor weight and height velocities (Fig. 2). Her biochemical profile was significant for hypophosphatemia as well as an inappropriately low tubular reabsorption of phosphate and an elevated serum 1,25(OH)$_2$D level (Table 1). In addition, serum C-terminal FGF23 was inappropriately normal in the context of hypophosphatemia, since the healthy, physiological response to low serum phosphate levels is a low serum FGF23 level.

At presentation, plain radiographs showed evidence of rickets plus bilateral lower limb bowing deformity (Fig. 3A), one proximal femoral transverse lucency consistent with a Looser zone (also known as a fracture or a pseudofracture in this context) (Fig. 3A), and two tibial cortical infractions also suggestive of osteomalacic fractures (Fig. 3B). To determine the extent of systemic osteomalacia resulting from hypophosphatemia, a trans-iliac biopsy was taken pre-burosumab from the unaffected contralateral side. The decision to biopsy the contralateral side was made in order to capture the extent of systemic, hypophosphatemia-related osteomalacia in an area where the bone was expected to be unaffected by the focal CSHS. In addition, the attending physician carrying out the procedure was concerned about exacerbating the already-inflamed nevi on the affected side. Her bone histomorphometry on the unaffected side demonstrated a mild mineralization defect with diffuse uptake of dual tetracycline label under fluorescent light (Fig. 4). The patient was diagnosed clinically with CSHS, given evidence of hypophosphatemic rickets due to renal phosphate-wasting, in conjunction with her linear sebaceous nevi. At the time of this publication, a pathogenic variant had not yet been identified in this patient.

2.2. Course of treatment with conventional therapy

Phosphate supplementation (Joulie's solution, 20 mg/kg/day) and calcitriol (17 ng/kg/day) were initiated at 2 years and 11 months of age, for a total of 8 months. On phosphate supplementation (up to 27 mg/kg/day) and calcitriol (up to 26 ng/kg/day), the patient did not achieve clinical and biochemical rickets remission. Furthermore, her height remained below the 3rd percentile, her weight was at the 25th percentile (Fig. 2), and serum phosphate levels improved but did not attain the normal range (Fig. 5A). The patient also had persistently high 1,25(OH)$_2$D levels (which should normalize with clinically significant improvements in serum phosphate levels), along with elevations in serum alkaline phosphatase (ALP) above the upper limit of normal for age and sex (Fig. 5B, C). Clinical and radiographic signs of bilateral genu varum persisted (Fig. 3C), although there was an improvement in her lower extremity mechanical axis deviation (Table 2). There was no improvement in the two tibial Looser zones on repeat radiographs (Fig. 3D), but healing of the proximal femoral Looser zone was observed (Fig. 3C). Given the inadequate clinical response to conventional therapy in the setting of an inappropriately normal FGF23 for the degree of hypophosphatemia, and in a condition known to be associated with FGF23 over-activity, the patient was transitioned to burosumab.

2.3. Course of treatment with burosumab

At the age of 3 years and 7 months, following a 1-week washout period during which the patient's conventional treatment was discontinued, she started burosumab 0.7 mg/kg subcutaneously every 2 weeks, similar to the standard dose for pediatric XLH (0.8 mg/kg, Product Monograph, March 15, 2023). On this dose, the serum phosphate level rose from 0.90 to 1.78 mmol/L (normal range for age and sex: 1.23–1.76 mmol/L), exceeding the upper limit of normal (Fig. 5A). As such, the burosumab dose was progressively de-escalated to 0.2 mg/kg every 2 weeks over a period of 26 months (Fig. 6) to achieve and then maintain normal serum phosphate levels on burosumab. Serum 1,25(OH)$_2$D and serum ALP levels rapidly normalized on burosumab (in contrast to the response to conventional therapy) (Fig. 5B, C). Serum ionized calcium and parathyroid hormone (PTH) remained within the normal range throughout her course of burosumab treatment (Fig. 5D, E).

After 26 months on burosumab, the patient's height surpassed the 3rd percentile, and the weight increased from the 25th to 50th percentile (Fig. 2). There was also clinical and radiological improvement in her lower limb deformity (Fig. 3E), with significant improvement in her lower extremity mechanical axis deviation bilaterally (benchmarked to the last measurement on conventional therapy) (Table 2). In addition, the proximal left tibia Looser zone completely healed, whereas only partial healing of the distal left tibial lesion was observed upon clinical assessment (Fig. 3F), but remained asymptomatic. On repeat radiographs after 26 months of treatment with burosumab, a new Looser zone of the left distal femur, which was not present on previous imaging, was

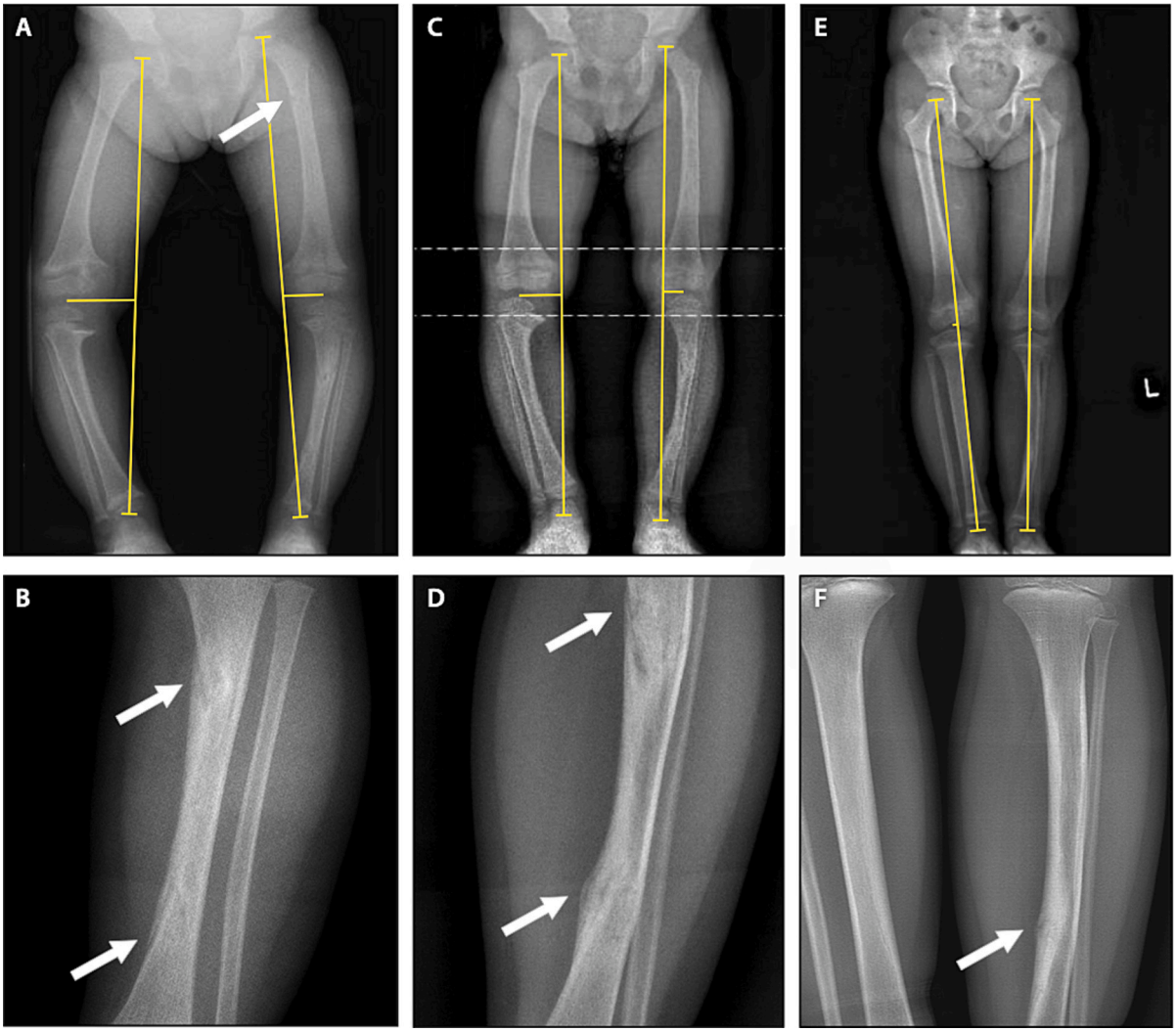

Fig. 3. X-rays of the patient's lower limb deformity, left proximal femoral Looser zone (A, C, E) and left tibia Looser zones (B, D, F) at diagnosis (A and B), 8 months into conventional treatment (C and D), and after 26 months of burosumab (E and F). The arrows indicate the locations of the Looser zones, and the lines represent the mechanical axis deviations.

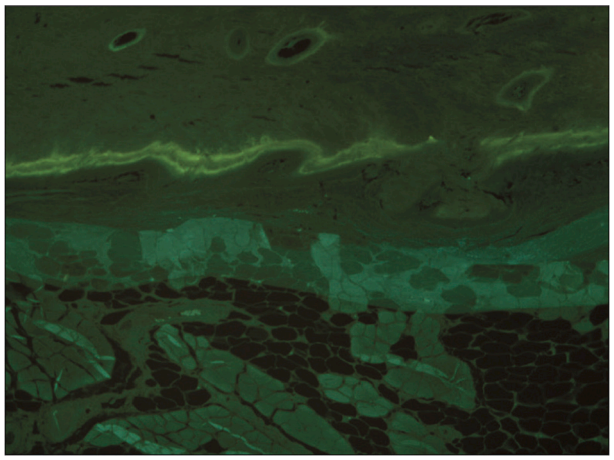

Fig. 4. Trans-iliac biopsy of the patient on the unaffected side prior to burosumab initiation, showing a mild mineralization defect with diffuse uptake of dual tetracycline label. Yellow lines represent bone tissue in which a dual tetracycline label was incorporated.

noted (Fig. 7A, B). The patient was asymptomatic, without any pain at the location of this new lesion. The new left distal femoral Looser zone was also confirmed by computerized tomography (Fig. 7C, D).

Burosumab was well-tolerated in this patient, who did not report any adverse effects related to the therapy at any time during the course of treatment.

3. Discussion

Here we describe the use of burosumab in an FGF23-mediated hypophosphatemia associated with CSHS. Our patient with CSHS overall responded well to burosumab, with clinical, biochemical and radiographic improvement of her physical signs, clinical symptoms and laboratory investigations associated with rickets, despite a small dose of burosumab. Burosumab was also well-tolerated.

3.1. Burosumab dosing

Burosumab has been approved by a number of health authorities worldwide for children with XLH who are six (or 12) months of age and older; it has also been approved by various health authorities for the treatment of tumor-induced osteomalacia. Interestingly, our patient's weight-based burosumab dose was lowered to under half of the starting

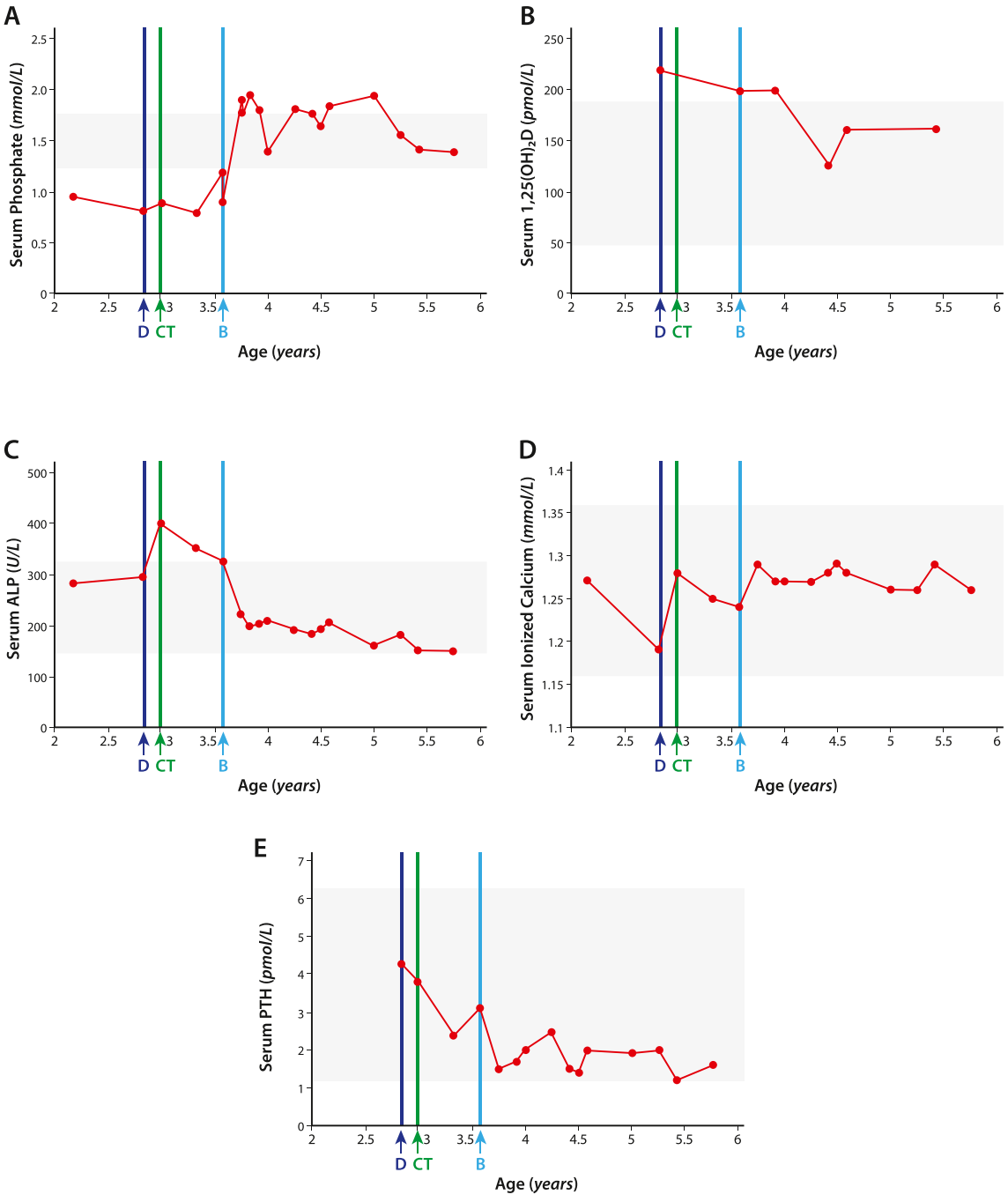

Fig. 5. Biochemical measurements over time. The time of diagnosis, the start of conventional therapy, and burosumab initiation are highlighted by purple, green, and light blue vertical lines, respectively. The gray area indicates the normative range of each parameter. Abbreviations: $1,25(OH)_2D$ = 1,25-dihydroxyvitamin D; ALP = alkaline phosphatase, PTH = parathyroid hormone.

Table 2
Lower limb deformity mechanical axis deviation at diagnosis, after 8 months on conventional treatment, and after 26 months on burosumab.

Disease timepoint	Mechanical axis deviation of the lower extremities (mm)	
	Right	Left
At diagnosis	49.5	28.6
After 8 months on conventional treatment	33.2	16.4
After 26 months on burosumab	5.0	1.0

dose for pediatric XLH, which may be due to the mild systemic osteomalacia (as noted on biopsy at diagnosis) that is in contrast to the more severe osteomalacia typical of XLH (Robinson et al., 2020). This observation is similar to the case published by Merz et al. wherein a 3-year-old girl with CSHS achieved normal serum phosphate and ALP levels, improved rickets, partial recovery of Looser zones, as well as increased mobility and quality of life, on a similarly low dose of burosumab (0.3–0.4 mg/kg every 2 weeks), after failing to heal on conventional therapy (Merz et al., 2022). Furthermore, Sugarman et al. reported two CSHS cases, one pediatric and one adult, which similarly

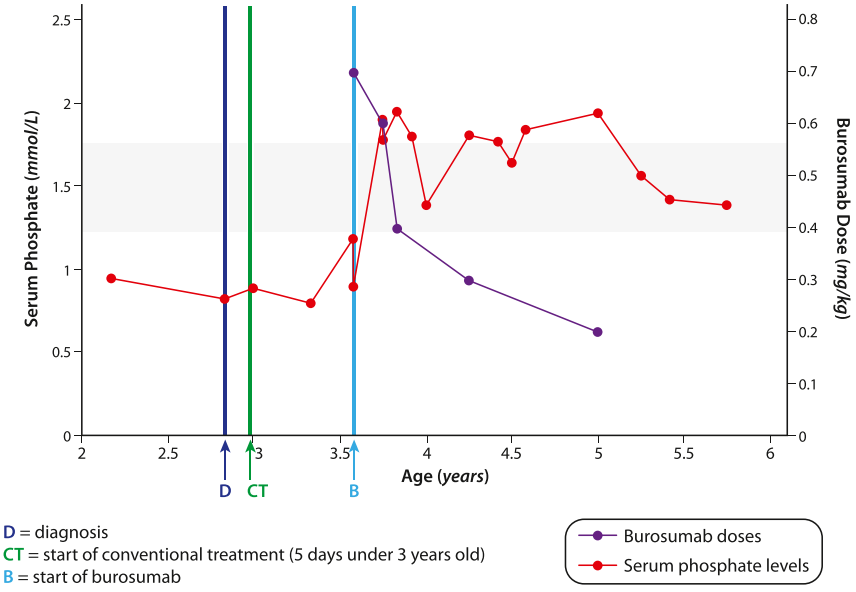

Fig. 6. Serum phosphate levels (red) in response to burosumab dose adjustment (purple) over time. The time of diagnosis, the start of conventional therapy, and burosumab initiation are highlighted by purple, green, and light blue vertical lines, respectively. The normal serum phosphate range is indicated by the gray region.

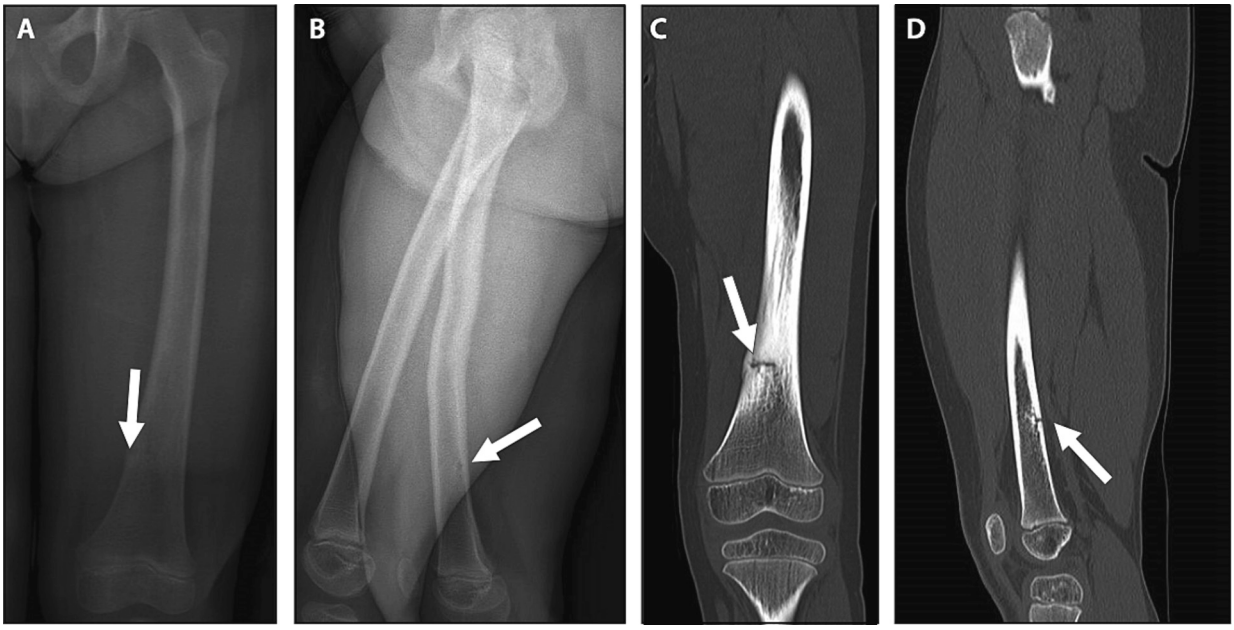

Fig. 7. Left distal femoral Looser zone noted after 26 months of burosumab on radiographs (A, B) and dedicated computerized tomography scan of the left femur (C, D). The arrows indicate the location of the Looser zone.

featured lower burosumab dosing (0.3 mg/kg every 3 weeks), with notable improvement in numerous parameters including serum phosphorous, limb deformities, fractures, mobility, and serum bone turnover markers (bone-specific ALP, procollagen 1 intact N-terminal propeptide, and C-terminal telopeptide of type 1 collagen) (Sugarman et al., 2023).

Unlike prior case reports of patients with CSHS, all of whom had elevations in serum FGF23 levels in cases where it was measured (Khadora and Mughal, 2021; Merz et al., 2022; Sugarman et al., 2023; Lim et al., 2014; Hoffman et al., 2005; Heike et al., 2005), our patient's FGF23 level was within the normal range at diagnosis. However, the normal physiologic response to hypophosphatemia is a low FGF23, in order to maximize renal phosphate reclamation in an effort to restore euphosphatemia. Inappropriately normal or high FGF23 levels have also been described in XLH (Weber et al., 2003). At this time, no clear cut-off value for serum C-terminal FGF23 in individuals with hypophosphatemia has been proposed to diagnose FGF23-related hypophosphatemia (such a cut-off value for C-terminal FGF23 level has only been published for tumor-induced osteomalacia (Hartley et al., 2022)). However, Hartley et al. suggest that C-terminal FGF23 values less than 45 RU/mL are 100% sensitive for FGF23-independent diseases, whereas levels between 45 and 90 RU/mL constitute a gray zone in which genetic FGF23-mediated disorders overlap with FGF23-independent forms of hypophosphatemia. Our patient's serum C-terminal FGF23 level was 63 RU/mL, which falls within this proposed gray zone. This observation, along with her other biochemical parameters of phosphate homeostasis, and her favourable response to burosumab, support that excessive FGF23 activity was responsible for our patient's hypophosphatemia.

Interestingly, our patient had a slightly high $1,25(OH)_2D$ level at diagnosis; similar observations have been made in other cases of linear sebaceous nevi with hypophosphatemic rickets (Feldmann et al., 1990; Oranje et al., 1994). Furthermore, our patient's elevation in serum $1,25(OH)_2D$ was considerably less than the very high levels described in hereditary hypophosphatemic rickets with hypercalciuria (HHRH) (Lorenz-Depiereux et al., 2006; Bergwitz and Miyamoto, 2019), which is a non-FGF23-mediated hypophosphatemic disorder arising from loss-of-function mutations in the gene encoding the sodium-dependent phosphate cotransporter 2c (*SLC34A3*). In HHRH, evidence for "functional $1,25(OH)_2D$ excess" beyond high $1,25(OH)_2D$ levels is found in the high urinary calcium/creatinine levels and frequent presence of nephrocalcinosis at diagnosis (Stürznickel et al., 2022). In contrast, our patient had a low-normal urinary calcium/creatinine despite a normal 25OHD level and adequate dietary intake of calcium and vitamin D. Together, these findings highlight that a slightly high $1,25(OH)_2D$ level does not rule out the presence of an FGF23-mediated hypophosphatemic condition, just as an inappropriately normal FGF23 level (as opposed to a frankly low level) does not definitely rule out an FGF23-mediated disorder (as demonstrated in patients with XLH) (Weber et al., 2003).

3.2. Healing of osteomalacic fractures

In our patient, treatment with burosumab led to significant improvement in lower limb deformity, pain, growth delay, full healing of one Looser zone (fracture), and partial of a second. In adults with XLH, Insogna and colleagues reported improved fracture healing on burosumab, with complete healing of 43% of fractures after 24 weeks compared with 7% on placebo (Insogna et al., 2018). Furthermore, there was ongoing healing of fractures over the next 24 weeks in both the burosumab and the placebo-to-burosumab cross-over groups (Portale et al., 2019).

While complete fracture healing has not yet been achieved in our patient after 26 months on burosumab, similar outcomes were observed in other CSHS cases, where Looser zones persisted after 12 months of burosumab therapy (Ovejero et al., 2016; Khadora and Mughal, 2021). Our patient also sustained a new femoral Looser zone despite maintaining euphosphatemia for 26 months on burosumab, suggesting that the underlying dysplastic bone may contribute to the fracture phenotype in CSHS. Whereas burosumab successfully restored euphosphatemia by neutralizing FGF23, its effect on dysplastic skeletal lesions remains unclear. Fracture healing in response to burosumab treatment in CSHS may differ from what has been observed in adult XLH given that, in addition to systemic osteomalacia, patients with CSHS also have focal dysplastic skeletal lesions (Heike et al., 2005; Lim et al., 2014). A bone biopsy of a focal bone lesion ipsilateral to the nevi in a patient with epidermal nevus syndrome and hypophosphatemia showed, in addition to osteomalacia, scattered areas of irregularly-shaped, poorly-defined lucencies, loss of cortical-medullary junctions, and linear areas of sclerosis (Heike et al., 2005). Histologic examination of dysplastic skeletal lesions in patients with CSHS by Lim and colleagues also showed fibroblast-like spindle-shaped cells surrounded by a dense collagen matrix (Lim et al., 2014). The focal dysplastic skeletal tissue may lack structural integrity which may evolve independently of restoring euphosphatemia with burosumab. Therefore, it is conceivable that persistent focal bone lesions in CSHS could hinder the fracture healing process and be associated with new Looser zones despite achieving euphosphatemia with burosumab, as demonstrated in our patient.

Another possibility is that incomplete osteomalacic fracture healing in CSHS could result from persistent tibial bowing and associated mechanical strain, which may ultimately necessitate surgical intervention to facilitate recovery by removing the strain (in this patient, on the medial aspect of the left tibia). Long-term follow-up is necessary to evaluate whether our patient will achieve complete fracture healing with or without limb-straightening surgical intervention. Another hypothesis to explain incomplete fracture healing in CSHS is dysregulation by *RAS* family pathogenic variants or other factors involved in the modulation of skeletal mineralization, such as osteopontin. Increased expression of osteopontin, a potent mineralization inhibitor, has been reported in murine models of XLH (Barros et al., 2013). Overexpression of osteopontin was also found through in-vitro studies in certain RASopathies, including neurofibromatosis type 1 and cardiofaciocutaneous syndrome (Choi et al., 2017; Fowlkes et al., 2021). While it remains unknown whether somatic *RAS*-family pathogenic variants dysregulate osteopontin expression in vivo, including in CSHS, one could hypothesize that, should this be the case in CSHS, mineralization defects caused by focal, excessive osteopontin secretion would impair fracture healing independently from FGF23 hypersecretion, and would not be targeted by burosumab therapy. Assessing osteopontin expression in biopsied tissues of nevi and dysplastic bone lesions could be the next step to explore this hypothesis further.

4. Conclusion and future directions

This case provides evidence for the use of burosumab in CSHS, a condition for which insights regarding treatment options are currently limited. Our findings open new paths of inquiry with respect to the use of burosumab for CSHS and other FGF23-mediated hypophosphatemic conditions (apart from X-linked hypophosphatemia and tumor-induced osteomalacia). Further studies evaluating the association between genetic mosaicism in CSHS and the skeletal phenotype are important to understand burosumab dose titration, clinical response, and monitoring of burosumab in this context.

Ethical approval and informed consent

This investigation was conducted in accordance with the Declaration of Helsinki. Written consent was obtained from the caregiver in line with the Children's Hospital of Eastern Ontario Research Institute's ethical requirements.

CRediT authorship contribution statement

Lillian Abebe: Writing – original draft, Visualization, Investigation, Data curation. **Kim Phung:** Writing – review & editing, Writing –

original draft, Supervision. **Marie-Eve Robinson:** Writing – review & editing, Supervision, Resources. **Richelle Waldner:** Writing – review & editing. **Sasha Carsen:** Writing – review & editing, Resources. **Kevin Smit:** Writing – review & editing, Resources. **Andrew Tice:** Writing – review & editing, Resources. **Joanna Lazier:** Writing – review & editing, Resources. **Christine Armour:** Writing – review & editing, Resources. **Marika Page:** Writing – review & editing, Resources. **Saunya Dover:** Writing – review & editing. **Frank Rauch:** Writing – review & editing, Data curation. **Khaldoun Koujok:** Writing – review & editing, Data curation. **Leanne M. Ward:** Writing – original draft, Validation, Supervision, Resources, Project administration, Methodology, Investigation, Funding acquisition, Conceptualization.

Declaration of competing interest

The authors declare no competing financial interests or conflicts of interest related to this study. Unrelated to this study, Dr. Ward declares consultancy to and participation in clinical trials with Ultragenyx, and consultancy to Kyowa Kyrin. Unrelated to this study, MER has been a consultant to Ultragenyx (with funds to Dr. Robinson's research program).

Data availability

Data will be made available on request.

Acknowledgements

LMW was supported by a Tier 1 Clinical Research Chair Award in Pediatric Bone Disorders from the University of Ottawa and the Children's Hospital of Eastern Ontario Research Institute. MER was supported by a Junior Clinical Research Chair Award from the University of Ottawa and by the Children's Hospital of Eastern Ontario Research Institute. We wish to thank the Bone Histomorphometry Unit of the Shriners Hospital for Children in Montreal, Canada, under Dr. Rauch, for performing the bone histomorphometric analyses.

References

Barros, N.M., Hoac, B., Neves, R.L., Addison, W.N., Assis, D.M., Murshed, M., Carmona, A.K., McKee, M.D., 2013. Proteolytic processing of osteopontin by PHEX and accumulation of osteopontin fragments in Hyp mouse bone, the murine model of X-linked hypophosphatemia. J. Bone Miner. Res. 28 (3), 688–699. https://doi.org/10.1002/jbmr.1766.

Bergwitz, C., Miyamoto, K.I., 2019. Hereditary hypophosphatemic rickets with hypercalciuria: pathophysiology, clinical presentation, diagnosis and therapy. Pflügers Arch. - Eur. J. Physiol. 471 (1), 149–163. https://doi.org/10.1007/S00424-018-2184-2.

Choi, J.Y., Han, K.M., Kim, D., Lee, B.H., Yoo, H.W., Choi, J.H., Han, Y.M., 2017. Impaired osteogenesis of disease-specific induced pluripotent stem cells derived from a CFC syndrome patient. Int. J. Mol. Sci. 18 (12) https://doi.org/10.3390/ijms18122591.

Feldmann, J.L., Enjolras, O., Penicaud, J.F., Menkès, C.J., 1990. Solomon's syndrome associated with fibrous dysplasia of bone and vitamin-resistant rickets. Rev. Rhum. Mal. Osteoartic. 57 (12), 881–884.

Fowlkes, J.L., Thrailkill, K.M., Bunn, R.C., 2021. RASopathies: the musculoskeletal consequences and their etiology and pathogenesis. Bone 152, 116060. https://doi.org/10.1016/j.bone.2021.116060.

Hartley, I.R., Gafni, R.I., Roszko, K.L., Brown, S.M., de Castro, L.F., Saikali, A., Ferreira, C.R., Gahl, W.A., Pacak, K., Blau, J.E., Boyce, A.M., Salusky, I.B., Collins, M. T., Florenzano, P., 2022. Determination of FGF23 levels for the diagnosis of FGF23-mediated hypophosphatemia. J. Bone Miner. Res. 37, 2174–2185. https://doi.org/10.1002/JBMR.4702.

Heike, C.L., Cunningham, M.L., Steiner, R.D., Wenkert, D., Hornung, R.L., Gruss, J.S., Gannon, F.H., McAlister, W.H., Mumm, S., Whyte, M.P., 2005. Skeletal changes in epidermal nevus syndrome: does focal bone disease harbor clues concerning pathogenesis? Am. J. Med. Genet. A 139a (2), 67–77. https://doi.org/10.1002/ajmg.a.30915.

Hoffman, W.H., Jueppner, H.W., DeYoung, B.R., O'Dorisio, M.S., Given, K.S., 2005. Elevated fibroblast growth factor-23 in hypophosphatemic linear nevus sebaceous syndrome. Am. J. Med. Genet. A 134, 233–236. https://doi.org/10.1002/AJMG.A.30599.

Imel, E.A., Glorieux, F.H., Whyte, M.P., Munns, C.F., Ward, L.M., Nilsson, O., Simmons, J.H., Padidela, R., Namba, N., Cheong, H.I., Pitukcheewanont, P., Sochett, E., Högler, W., Muroya, K., Tanaka, H., Gottesman, G.S., Biggin, A., Perwad, F., Mao, M., Chen, C.Y., Skrinar, A., San Martin, J., Portale, A.A., 2019. Burosumab versus conventional therapy in children with X-linked hypophosphataemia: a randomised, active-controlled, open-label, phase 3 trial. Lancet 393 (10189), 2416–2427. https://doi.org/10.1016/s0140-6736(19)30654-3.

Insogna, K.L., Briot, K., Imel, E.A., Kamenický, P., Ruppe, M.D., Portale, A.A., Weber, T., Pitukcheewanont, P., Cheong, H.I., Jan de Beur, S., Imanishi, Y., Ito, N., Lachmann, R.H., Tanaka, H., Perwad, F., Zhang, L., Chen, C.Y., Theodore-Oklota, C., Mealiffe, M., San Martin, J., Carpenter, T.O., 2018. A randomized, double-blind, placebo-controlled, phase 3 trial evaluating the efficacy of Burosumab, an anti-FGF23 antibody, in adults with X-linked hypophosphatemia: week 24 primary analysis. J. Bone Miner. Res. 33 (8), 1383–1393. https://doi.org/10.1002/jbmr.3475.

Khadora, M., Mughal, M.Z., 2021. Burosumab treatment in a child with cutaneous skeletal hypophosphatemia syndrome: a case report. Bone Rep. 15, 101138 https://doi.org/10.1016/j.bonr.2021.101138.

Lim, Y.H., Ovejero, D., Sugarman, J.S., Deklotz, C.M., Maruri, A., Eichenfield, L.F., Kelley, P.K., Jüppner, H., Gottschalk, M., Tifft, C.J., Gafni, R.I., Boyce, A.M., Cowen, E.W., Bhattacharyya, N., Guthrie, L.C., Gahl, W.A., Golas, G., Loring, E.C., Overton, J.D., Mane, S.M., Lifton, R.P., Levy, M.L., Collins, M.T., Choate, K.A., 2014. Multilineage somatic activating mutations in HRAS and NRAS cause mosaic cutaneous and skeletal lesions, elevated FGF23 and hypophosphatemia. Hum. Mol. Genet. 23 (2), 397–407. https://doi.org/10.1093/hmg/ddt429.

Lim, Y.H., Ovejero, D., Derrick, K.M., Collins, M.T., Choate, K.A., 2016. Cutaneous skeletal hypophosphatemia syndrome (CSHS) is a multilineage somatic mosaic RASopathy. J. Am. Acad. Dermatol. 75 (2), 420–427. https://doi.org/10.1016/j.jaad.2015.11.012.

Lorenz-Depiereux, B., Benet-Pages, A., Eckstein, G., Tenenbaum-Rakover, Y., Wagenstaller, J., Tiosano, D., Gershoni-Baruch, R., Albers, N., Lichtner, P., Schnabel, D., Hochberg, Z., Strom, T.M., 2006. Hereditary hypophosphatemic rickets with hypercalciuria is caused by mutations in the sodium-phosphate cotransporter gene SLC34A3. Am. J. Hum. Genet. 78, 193–201. https://doi.org/10.1086/499410.

Merz, L.M., Buerger, F., Ziegelasch, N., Zenker, M., Wieland, I., Lipek, T., Wallborn, T., Terliesner, N., Prenzel, F., Siekmeyer, M., Dittrich, K., 2022. A case report: first long-term treatment with Burosumab in a patient with cutaneous-skeletal hypophosphatemia syndrome. Front. Endocrinol. (Lausanne) 13, 866831. https://doi.org/10.3389/fendo.2022.866831.

Oranje, A.P., Przyrembel, H., Meradji, M., Loonen, M.C.B., de Klerk, J.B.C., 1994. Solomon's epidermal nevus syndrome (type: linear nevus Sebaceus) and hypophosphatemic vitamin D—resistant rickets. Arch. Dermatol. 130, 1167–1171. https://doi.org/10.1001/archderm.1994.01690090091013.

Ovejero, D., Lim, Y.H., Boyce, A.M., Gafni, R.I., McCarthy, E., Nguyen, T.A., Eichenfield, L.F., DeKlotz, C.M., Guthrie, L.C., Tosi, L.L., Thornton, P.S., Choate, K. A., Collins, M.T., 2016. Cutaneous skeletal hypophosphatemia syndrome: clinical spectrum, natural history, and treatment. Osteoporos. Int. 27 (12), 3615–3626. https://doi.org/10.1007/s00198-016-3702-8.

Ovejero, D., Michel, Z., Cataisson, C., Saikali, A., Galisteo, R., Yuspa, S.H., Collins, M.T., de Castro, L.F., 2023. Murine models of HRAS-mediated cutaneous skeletal hypophosphatemia syndrome suggest bone as the FGF23 excess source. J. Clin. Invest. 133 (9) https://doi.org/10.1172/jci159330.

Portale, A.A., Carpenter, T.O., Brandi, M.L., Briot, K., Cheong, H.I., Cohen-Solal, M., Crowley, R., Jan De Beur, S., Eastell, R., Imanishi, Y., Imel, E.A., Ing, S., Ito, N., Javaid, M., Kamenicky, P., Keen, R., Kubota, T., Lachmann, R., Perwad, F., Pitukcheewanont, P., Ralston, S.H., Takeuchi, Y., Tanaka, H., Weber, T.J., Yoo, H. W., Zhang, L., Theodore-Oklota, C., Mealiffe, M., San Martin, J., Insogna, K., 2019. Continued beneficial effects of Burosumab in adults with X-linked hypophosphatemia: results from a 24-week treatment continuation period after a 24-week double-blind placebo-controlled period. Calcif. Tissue Int. 105 (3), 271–284. https://doi.org/10.1007/s00223-019-00568-3.

Robinson, M.E., AlQuorain, H., Murshed, M., Rauch, F., 2020. Mineralized tissues in hypophosphatemic rickets. Pediatr. Nephrol. 35, 1843–1854. https://doi.org/10.1007/S00467-019-04290-Y/FIGURES/4.

Stürznickel, J., Heider, F., Delsmann, A., Gödel, M., Grünhagen, J., Huber, T.B., Kornak, U., Amling, M., Oheim, R., 2022. Clinical spectrum of hereditary hypophosphatemic rickets with hypercalciuria (HHRH). J. Bone Miner. Res. 37, 1580–1591. https://doi.org/10.1002/JBMR.4630.

Sugarman, J., Maruri, A., Hamilton, D.J., Tabatabai, L., Luca, D., Cimms, T., Krolczyk, S., Roberts, M.S., Carpenter, T.O., 2023. The efficacy and safety of burosumab in two patients with cutaneous skeletal hypophosphatemia syndrome. Bone 166, 116598. https://doi.org/10.1016/j.bone.2022.116598.

Weber, T.J., Liu, S., Indridason, O.S., Quarles, L.D., 2003. Serum FGF23 levels in Normal and disordered phosphorus homeostasis. J. Bone Miner. Res. 18, 1227–1234. https://doi.org/10.1359/JBMR.2003.18.7.1227.